Theory and Design of Fractional–Slot Multilayer Windings

Luigi Alberti, Nicola Bianchi

Department of Electrical Engineering,
University of Padova, ITALY
luigi.alberti@unipd.it, bianchi@die.unipd.it

***Abstract*—This paper deals with fractional–slot multilayer windings. They are becoming attractive since they allow to reduce the harmonic content of the windings magneto motive force. Some examples of such a type of windings are reported in literature, but they are limited to a few slot/pole combinations. On the contrary, in this paper the general theory is presented. General rules for the design of multilayer windings are illustrated.**

It is also investigated when the adoption of a multilayer winding makes possible to limit the torque ripple and the rotor losses of the machine. Several examples and experimental tests are reported to investigate the advantages and convenience of adopting multilayer windings.

***Index Terms*—Fractional slot windings, Multilayer windings, AC Machines, Electrical drive**

I. Introduction

Fractional slot (FS) windings are becoming more and more attractive solutions in many applications, for example in low speed high torque machines. Due to the low number of slots per pole and per phase, FS windings are characterized by a high MMF space harmonic content. Usually a winding is arranged so as to realize the maximum winding factor for the main harmonic, that is the harmonic of order $\nu' = p$ where p is the number of pole pairs. Typically single layer and double layer windings, i.e. with one or two layers, are considered in literature [1], [2]. Even though the various solutions exhibit a similar winding factor for the main harmonic, they exhibit different characteristics since their MMF harmonic content is different. Therefore, their performance is also different.

In order to reduce the amplitude of the MMF harmonics, it is possible to increase the number of layers in the winding [3], [4]. There are some examples in literature, but they are limited to few slot/pole combinations [5]–[7]. The aim of this paper is to present the general theory of multilayer m–phase windings. Moreover, the rules to layout such a type of windings are given. The feasibility criteria and the convenience to adopt a multilayer winding for the reduction of MMF harmonics amplitude are discussed. The general case of m–phase winding will be considered and example about 3– and 5–phase machines are included.

Several examples regarding different machine types are included in the paper together with experimental tests. At last, an application example is presented: a multilayer winding is adopted in a SPM machine. The convenience of adopting multilayer windings for each considered example is analyzed and discussed.

II. Design of balanced symmetrical multiphase windings

The procedure based on the star of slots theory [1], [2], [8] is used to design a balanced and symmetrical m–phase winding. The machine periodicity t is defined as the greatest common divisor (GCD) between the slots number Q and the pole pairs:

$$t = GCD\{Q, p\} \tag{1}$$

The number of spokes in the star of slots is Q/t. The angle between two spokes is

$$\alpha_{ph} = 360\ t/Q \quad \text{degrees} \tag{2}$$

The star of slots is divided in $2 \cdot m$ sectors, each of them spanning $360/(2\ m)$ degrees. Two opposite sectors are assigned to each phase. The two sectors are referred to as positive (e.g. labeled A+) and negative sectors (e.g. labeled A-), and they are drawn on the star of slots with a displacement of 180 degrees, see Fig. 1(a). The number of spokes in each sector is $Q/(2\ m\ t)$. Two examples in the case of 3–phase winding are reported in Fig. 1 and Fig. 2. The star of slots is drawn with the six sectors (two for each phase). The positive sectors are labeled as A+,B+ and C+; similarly, for the negative sectors the letters A-,B- and C- are used. As regards the number of spokes per phase in the star of slots, there are two cases to be considered:

- When Q/t is an even number the number of spokes in the positive sector is the same as the number of spokes in the negative sector, as in Fig. 1(a);
- When Q/t is an odd number the number of spokes in the positive sectors differs by 1 respect to the number of spokes in the negative sector, as in Fig. 2(a).

III. Layout of 2–layer windings

Once the phase sectors are drawn, it is possible to assign the coil of each phase to the corresponding slots. The coil throw is computed as

$$y_q = round\{Q/(2p)\} \tag{3}$$

As an example, referring to Fig. 1(a), 4 slots are assigned to the phase A, one for each spoke of the star (i.e. number 1, 6, 7 and 12). In the slots of the positive sector (1 and 6) is located a coil side with positive (incoming) incidence. Then the other coil sides are located according to the computed coil throw, i.e. in the slot 2 and 7 with $y_q = 1$. In this way the two coils of the positive sectors A+

978-1-4577-0541-0/11/$26.00 ©2011 IEEE

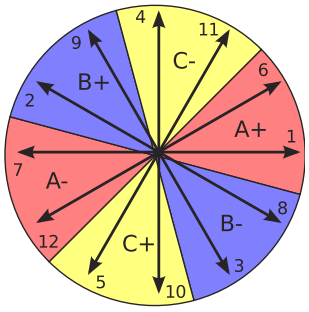

(a) Star of slots

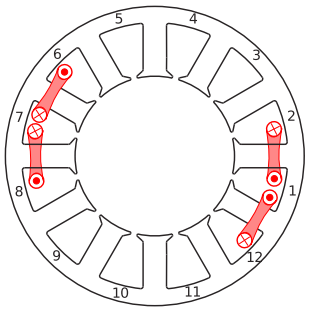

(b) Winding layout of phase A

Fig. 1. 12–slot 10–pole, 2–layer winding, three–phase machine

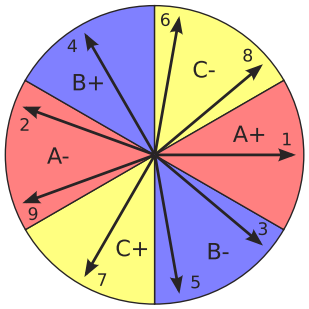

(a) Star of slots

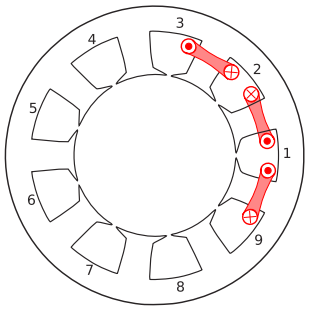

(b) Winding layout of phase A

Fig. 2. 9–slot 8–pole, 2–layer winding, three–phase machine

are located in the slots 1–2 and 6–7. The two coils of the negative sector A- are located similarly but with inverse incidence. So that they are located in the slot 8–7, 1–12 (the first number is the slot with a positive incidence (8 and 1) and the second number is the slot with a negative incidence (7 and 12)).

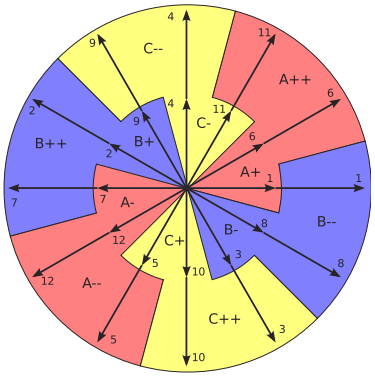

(a) Star of slots

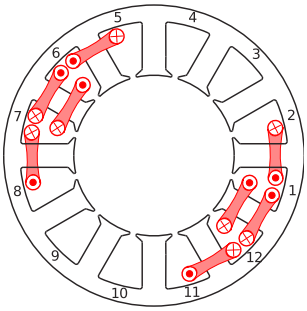

(b) Winding layout of phase A

Fig. 3. 12–slot 10–pole, 4–layer winding, α_{sh4}=α_{ph}, three–phase machine

IV. Layout of 4–layer windings

In order to design a 4–layer winding, the sectors are doubled. Therefore each phase has two positive and two negative sectors. The positive sectors for the phase are indicated as A+ and A++. The negative sectors are indicated as A- and A--. A similar notation is adopted for the phases B and C. Then, the second set of sectors is shifted on the star of slots of the angle α_{sh4}. Starting from the star of slots of Fig. 1(a), Fig. 3(a) shows the star of slots redrawn in the case of 4–layer winding.

A. Selection of the shift angle α_{sh4}

The selection of the shift angle α_{sh4} between the two sets of sectors is an additional degree of freedom in the winding design. In order to maximize the distribution factor for the main harmonic, the shift must be as small as possible. Two distinct case have to be considered depending on Q/t is an even or odd number.

1) Q/t even: When the ratio Q/t is an even number, the number of spokes in the positive and negative sectors is the same. Then, all positive and negative sectors of all phases contains the same number of spokes. For example, this is the case of the 12–slot 10–pole winding which star of slots is reported in Fig. 3(a). In order to obtain the maximum distribution factor for the main harmonic of order $\nu' = p$ the shift angle is equal to the angle between two spokes, that is $\alpha_{sh4} = \alpha_{ph}$. The corresponding winding layout is reported in Fig. 3(b).

2) Q/t odd: When Q/t is an odd number the number of spokes in the positive sectors differs by 1 with respect

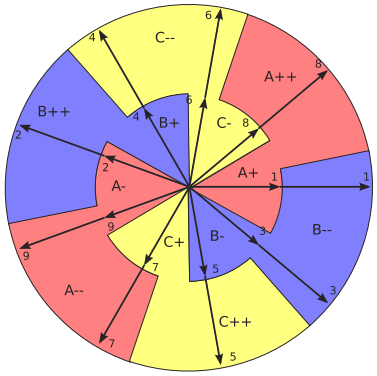

(a) Star of slots

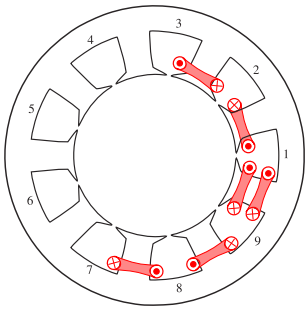

(b) Winding layout of phase A

Fig. 4. 9–slot 8–pole, 4–layer winding, solution i with α_{sh4}=α_{ph}

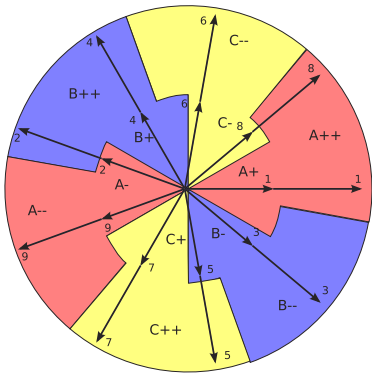

(a) Star of slots

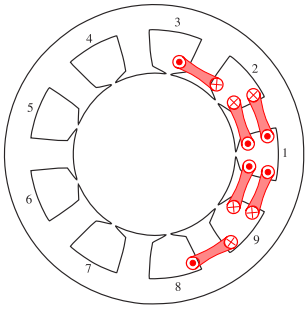

(b) Winding layout of phase A

Fig. 5. 9–slot 8–pole, 4–layer winding, solution ii with α_{sh4}=$\alpha_{ph}/2$

to the spokes number in the negative sector. Then it is possible to shift the sectors in two different ways as shown in Figs. 4(a) and 5(a). In the first case, Fig. 4(a), the shift angle is equal to the angle between two spokes, that is $\alpha_{sh4} = \alpha_{ph}$. In both the positive sectors A+ and A++ there is only one spoke, and in both the negative sectors A- and A-- there are two spokes.

The second possibility is shown in Fig. 5(a): the shift angle is equal to half the angle between two spokes, that is $\alpha_{sh4} = \alpha_{ph}/2$. There is only one spoke in the sector A+ and there are two spokes in the sector A++. In this second case, a higher distribution factor is expected for the main harmonic of order $\nu' = p$ since the spokes of the coils connected in series are closer respect to the case of Fig. 4(a). For both cases the winding layouts is reported in Fig. 4(b) and Fig. 5(b) an example of these configuration is reported also in [6]. The winding factors for different MMF harmonic order are shown in Table. I.

For the main harmonic of order $\nu' = p$ the winding factor of the 4–layer winding, can be computed starting from that of the 2–layer winding as:

$$k_{w4} = k_{w2} \frac{\sin \alpha_{sh4}}{2 \sin \frac{\alpha_{sh4}}{2}} \tag{4}$$

where α_{sh4} is the selected shift angle between the two sets of sectors.

B. Limitations in adopting a 4–layer winding

A 4–layer winding is always feasible in the sense of increasing up to 4 the number of the coil sides in the slots. Nevertheless the 4–layer windings are not convenient for

TABLE I
WINDING FACTORS FOR 9–SLOT 8–POLE WINDINGS

ν'	2–layer Fig 2(a)	4–layer i Fig 4(a)	4–layer ii Fig 5(a)
1	0.061	0.046	0.021
2	0.139	0.024	0.090
4	**0.945**	**0.888**	**0.931**
5	0.945	0.888	0.931
7	0.139	0.024	0.090
8	0.061	0.046	0.021
10	0.061	0.046	0.021
11	0.139	0.024	0.090

every combinations of slots and poles. The star of slots helps in understanding this fact.

In order to realize a 4 layer windings it is necessary that each phase has at least two spokes in one sector of the star of slots. Since the number of spokes per phase is $Q/(m\ t)$ and each phase has two sectors, the 4–layer winding is feasible if $Q/(2\ m\ t) > 1$.

For instance, a 3–phase machine with $Q/(2p) = 3/2$ has the star of slots with 3 spokes, that is, there is only one spoke in each positive sectors. In this case the decreasing of the amplitude is the same for all the MMF space–harmonics and so to adopt a 4–layer winding makes no sense.

C. Five–phase winding example

The considerations reported above are general and can be applied to any m–phase winding. As an example, the star of slots for the 4–layer winding of a 5–phase 15–slot 14–pole is reported in Fig. 6. In this case Q/t=15 is an odd

number and so two shift angles α_{sh4} can be considered. Fig. 6(a) shows the star of slots for $\alpha_{sh4} = \alpha_{ph}$, and Fig. 6(b) shows the star of slots for $\alpha_{sh4} = \alpha_{ph}/2$.

The winding layout can be derived according to the star of slots as above.

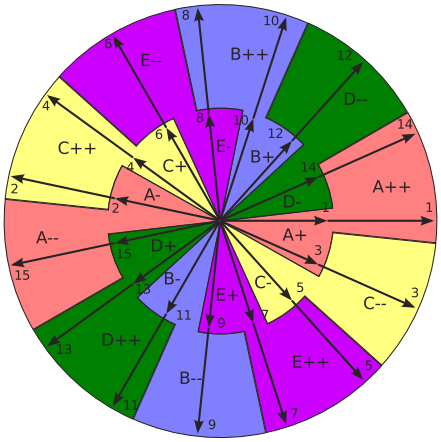

(a) 15–slot 14–pole, 4–layer winding, solution i with $\alpha_{sh4} = \alpha_{ph}$

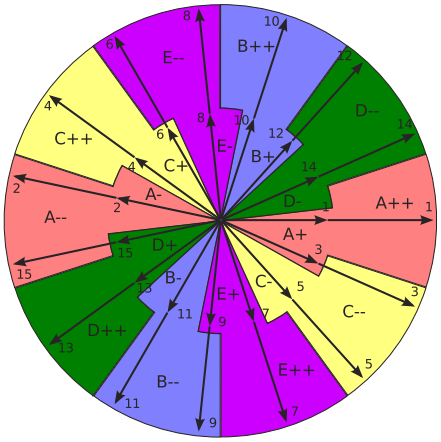

(b) 15–slot 14–pole, 4–layer winding, solution ii with $\alpha_{sh4} = \alpha_{ph}/2$

Fig. 6. Star of slots of the 5–phase 15–slot 14–pole 4–layer winding

D. Higher number of layers

The number of layers is not limited to 4 but it can be increased. An example of higher number of layers is reported in [6] where an interesting arrangement of the coils is presented. In general, to layout a l layer winding, $l/2$ set of 2 m sectors have to be considered in the star of slots.

V. Examples and Applications

The performance of an electrical machine strongly depends on the MMF harmonic content. It is shown in Table I that the adoption of a 4–layer winding is a means to reduce significantly the MMF harmonic content so as to improve the machine performance.

In this section some examples are given showing the advantages and drawbacks in adopting multilayer windings.

A. 9–slot 8–pole SPM machine

At first an SPM machine with 9 slots and 8 poles is considered. Such a machine is considered with three different windings: the 2–layer winding, the 4–layer winding solution i of Fig. 4(b) and the 4–layer winding solution ii of Fig. 5(b).

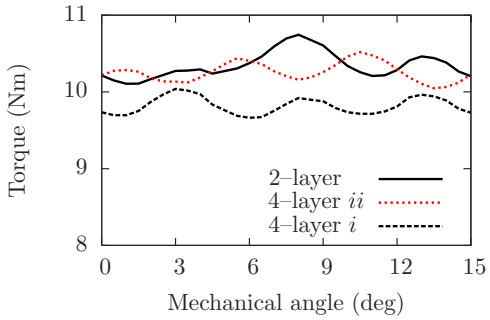

Fig. 7. Torque versus rotor position computed by means of finite element simulations: 9–slot 8–pole winding with different number of layers

TABLE II
Computed average torque and torque ripple for the characteristic of Fig. 7

Configuration	Average torque (Nm)	Torque ripple %
2–layer	10.3	6.2
4–layer i	9.8	3.8
4–layer ii	10.3	4.6

Fig. 7 shows the torque versus rotor position computed by means of finite element simulations. The computed average torque and torque ripple are reported in Table II. As can be noted the winding 4–layer solution i of Fig. 4(b) exhibits a slightly lower average torque due to the lower winding factor (see Table I). Then, the torque ripple for the 4–layer windings is lower. In particular the winding 4–layer solution i exhibits the lowest torque ripple.

B. Experimental results

A prototype available in the laboratory has been tested. It is an axial flux (AxF) SPM machine. It is provided by different rotors and stators which allow to consider various machine configurations. In particular, two rotors are adopted in the following, a normal rotor with magnetized PMs, and a solid iron rotor without PMs. This allows to investigate the rotor losses due to MMF harmonics as described in [9]. Then, two different stators are adopted. The first is characterized by a 1–layer winding as shown in Fig. 8. The second is shown in Fig. 9. Reconnecting properly the coils of the latter stator it is possible to test the machine with both 2– and 4–layer windings.

1) Back Electromotive Force: The back electromotive forces (BEMFs) have been measured at various speeds. The waveforms for the 2–layer winding at 1000 rpm are reported in Fig. 10. As expected for the 12–slot 10–pole configuration, the waveforms are very close to an ideal sinusoidal waveform. For the other number of layers similar waveforms are obtained and they are no included here.

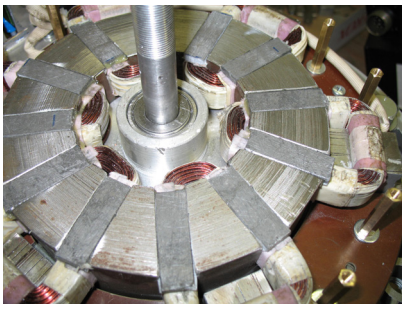

Fig. 8. The stator of the AxF SPM machine prototype with the 1–layer winding

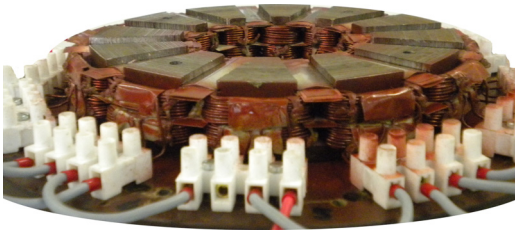

Fig. 9. A photo of the AxF SPM machine prototype with the 4–layer winding

The measured RMS values of the BEMFs are reported in Table III. As expected, increasing the number of layers, there is a slight reduction of the BEMF. This is due to the reduction of the winding factor of the main harmonic, according to (4).

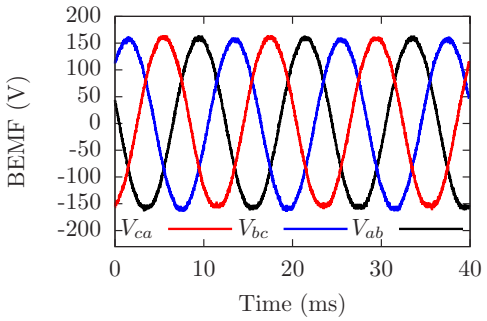

Fig. 10. Waveforms of the BEMF with the 2–layer winding at 1000 rpm

TABLE III
EXPERIMENTAL RESULT. PHASE–TO–PHASE BEMF (VRMS)

speed	1–layer	2–layer	4–layer
250 rpm	29.6	29.2	28.7
500 rpm	59.1	58.4	57.3
1000 rpm	114.6	113.7	109.3

2) Torque ripple measurements: In this test, the AxF SPM machine is tested under load. The machine is mounted on a test bench which imposes the mechanical speed. The bench rotates at very low speed. Then, the AxF SPM machine is supplied by an inverter with different currents and the torque is measured by means of a torque meter.

All the three numbers of winding layers are considered in the test. The measured torque versus the mechanical rotor position is shown in Fig. 11 for the 1–layer winding and in Fig. 12 and Fig. 13 for the 2– and 4–layer winding respectively.

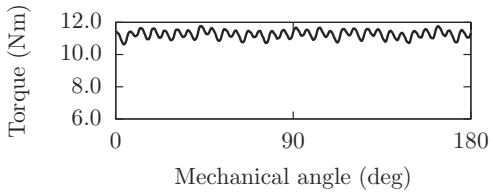

Fig. 11. Experimental test. Torque ripple of AxF SPM machine with 1–layer winding ($\hat{I}$=8 A)

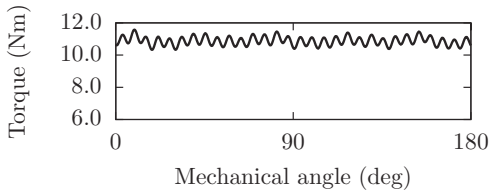

Fig. 12. Experimental test. Torque ripple of AxF SPM machine with 2–layer winding ($\hat{I}$=8 A)

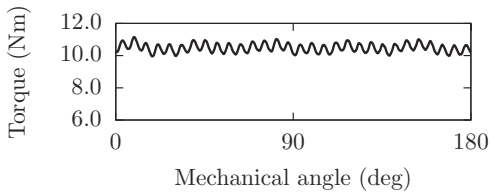

Fig. 13. Experimental test. Torque ripple of AxF SPM machine with 4–layer winding ($\hat{I}$=8 A)

The average torque τ_{avg} and the torque ripple $\Delta\tau$ for all the test are reported in Tables IV, V and VI for various current levels.

TABLE IV
TORQUE RIPPLE MEASUREMENT WITH 1–LAYER WINDING

$\hat{I}$ (A)	τ_{avg} (Nm)	$\Delta\tau$ (Nm)
1	1.27	1.06
2	2.72	1.07
4	5.59	1.06
6	8.43	1.08
8	11.25	1.18

As expected, the average torque increases with the current. Then a reduction of the average torque, according to (4) is present as the number of layers increases.

As far as the torque ripple is concerned, it is mainly due to the cogging. In fact it is almost the same for all the currents and with different numbers of layers. This is more clear considering Table VII where the results of measurements for the three number of layers are compared. The

TABLE V
TORQUE RIPPLE MEASUREMENT WITH 2–LAYER WINDING

$\hat{I}$ (A)	τ_{avg} (Nm)	$\Delta\tau$ (Nm)
1	1.22	1.14
2	2.62	1.15
4	5.38	1.15
6	8.13	1.24
8	10.88	1.28

TABLE VI
TORQUE RIPPLE MEASUREMENT WITH 4–LAYER WINDING

$\hat{I}$ (A)	τ_{avg} (Nm)	$\Delta\tau$ (Nm)
1	1.17	1.13
2	2.51	1.13
4	5.18	1.14
6	7.83	1.21
8	10.48	1.23

harmonic contents of the torque ripple has been computed and it is also reported in the first column of Table VII.

The last row highlighted in boldface is the main harmonic of torque ripple. As can be noted it is the dominant contribution for all the configurations. In fact, the torque harmonic of order 60 is the harmonic of the cogging torque. Its order is computed [10] as:

$$Q \cdot \frac{2p}{HCF\{2p, Q\}} = 12 \cdot 5 = 60 \tag{5}$$

Since the cogging torque is due to the interaction of PMs and stator slots, it is independent from the current and from the winding configuration.

TABLE VII
EXPERIMENTAL TEST. HARMONIC CONTENT OF TORQUE RIPPLE FOR VARIOUS NUMBER OF WINDING LAYER. $\hat{I}$=8 A

	1–layer	2–layer	4–layer
τ_{avg} (Nm)	11.25	10.88	10.48
$\Delta\tau$ (Nm)	1.18	1.28	1.23
$\Delta\tau$%	10.5	11.7	11.7
torque harmonic	torque harmonic amplitude % of mean value		
5	0.504	0.429	0.408
10	0.741	1.196	1.260
12	0.401	0.360	0.364
20	0.000	0.376	0.394
24	0.538	0.534	0.531
60	**2.575**	**2.830**	**2.795**

3) Rotor losses: Rotor losses in PM machine is an important issue since they can cause a considerable reduction of the overall drive performance [9], [11]–[13]. In particular, this is the case of machines where the PMs are not segmented or in machines with a solid iron yoke.

A large amount of rotor losses can be caused by stator MMF space harmonics and, therefore, they increase with the load. The stator space MMF harmonics move asynchronously with the rotor, inducing currents in all rotor conductive parts. Particularly significant for the rotor losses are the sub–harmonics of order $\nu' < p$ [11]. They have a high wavelength and, therefore, the corresponding flux lines enter deeply in the rotor. Moreover, rotor losses increase with the rotor speed.

Following the procedure described in [9] the rotor losses have been measured on the prototype with the three number of layers. The experimental results are reported in Fig. 14, considering the normal operation under load of the machine with a stator current $\hat{I}$=8 A. The rotor losses are due to both MMF harmonics and slot openings which interact with the PM flux. As expected, the 1–layer winding exhibits the higher losses. Then the rotor losses of the 2– and 4–layer windings are very close. This is explained considering that the main rotor losses under load are, in the prototype under test, due to the slot openings and due to the sub–harmonic of order $\nu' = 1$. The PM flux limits the impact of the MMF sub–harmonic on the rotor losses [11]. Then a significant reduction of the sub–harmonic occurs switching from the 1–layer winding to the 2–layer winding. A further reduction, of the sub–harmonic of order $\nu' = 1$ occurs considering a 4–layer winding. Anyway this reduction seems to give no reduction in the rotor losses of the prototype, probably due to the interaction of the sub–harmonic with the PMs flux.

This is confirmed in Fig. 15 which shows the rotor losses measured considering a solid iron rotor disk without PMs. In this case, the PMs flux lines are not present and the MMF harmonics can enter in the rotor yoke without encountering the path saturated by the PM flux. Therefore higher rotor losses are expected, as confirmed in Fig. 15. In this case, the rotor losses of the 2– and 4–layer configurations are lower, being, respectively, 31% and 20% of the losses with the the 1–layer configuration.

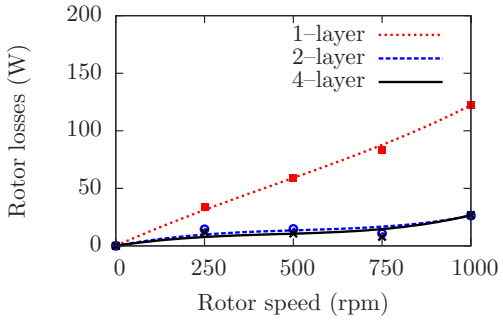

Fig. 14. Experimental test. Rotor losses under load with different number of layer

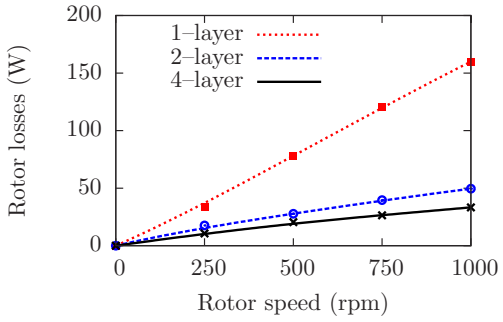

Fig. 15. Experimental test. Rotor losses with only iron in the rotor

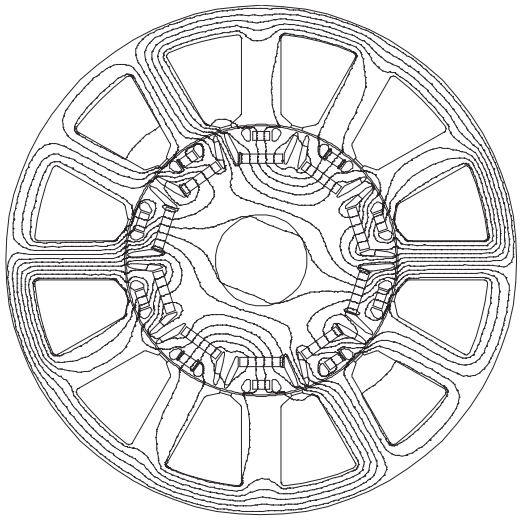

Fig. 16. Geometry and flux lines of the considered 12–slot 10–pole IPM machine

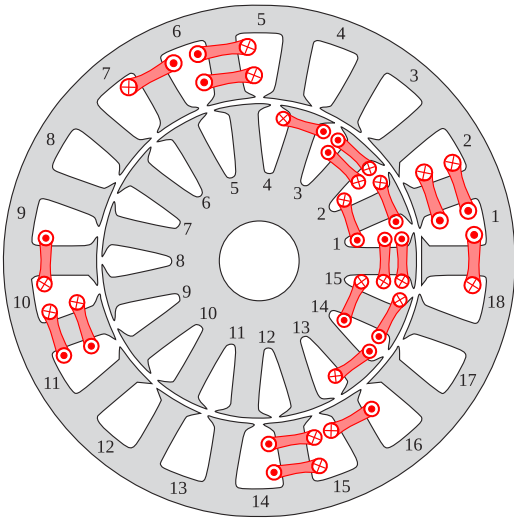

Fig. 18. 4–layer winding FS doubly fed IM. Lamination geometry and winding layout of one phase [16]

C. IPM machine

In this section an interior permanent magnet (IPM) machine is considered. It is a FS machine, characterized by 12 slots and 10 poles. The machine geometry is shown in Fig. 16 together with flux lines under load operation.

The motor is supplied with a peak current of 9 A on the maximum torque per Ampere trajectory. Fig. 17 shows the torque versus rotor angle computed by means of FE simulations. The average torque, torque ripple and the percentage torque ripple are reported in Table VIII.

With the IPM machine the average torque is almost the same for the three configurations. In such a machine, iron saturation can cause slight variations of the average torque. This is particular the case of fractional–slot machines [14]. It is reasonable that the 1–layer winding exhibits a lower torque since it has the highest amplitude of the MMF sub–harmonic of order $\nu' = 1$, and so higher saturation.

On the contrary, the torque ripple decreases significantly considering the 4–layer winding. This shows that the adoption of multilayer windings in IPM machines can be considered as an effective solution to improve the torque characteristic.

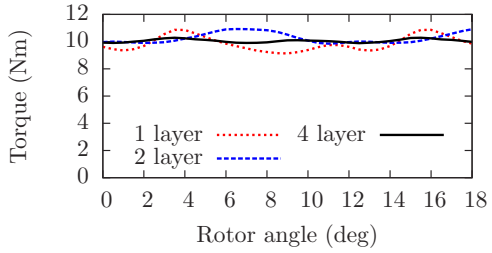

Fig. 17. Torque versus rotor position of IPM machine with different number of layer

D. Fractional slot induction machine

In this subsection a fractional slot wound–rotor induction machine (FSIM) is considered. It is characterized by two fractional–slot windings, the first in the stator and the second on the rotor [15]. The stator winding is supposed connected to the grid. A current control is assumed in the rotor winding so that both stator and rotor currents are sinusoidal.

Currently, these authors are investigating the feasibility of such a machine which design is quite challenging for its peculiarity. A draw of the considered lamination is shown in Fig. 18. It is characterized by 18 slots in the stator and 15 slots in the rotor. The selected number of poles is $2p$=14. In Fig. 18 it is also reported the winding layout of one phase for the 4–layer windings.

The actual torque is given by the interaction of all stator and rotor MMF harmonics that have the same harmonic order. To the aim of limiting the torque ripple, it is important to reduce the amplitude of all MMF harmonics whose order ν' is different from p. In this case a multilayer winding can be profitably adopted. More information about the FSIM and its detailed design can be found in [16].

The analytically computed torque versus rotor positions is reported in Fig. 19 for two different currents. The currents are imposed in both the stator and rotor. The rotor current vector angle is selected so as to maximize the torque per Ampere ratio.

The average torque, the torque ripple and the percentage

TABLE VIII
FE SIMULATIONS, IPM MACHINE. HARMONIC CONTENT OF TORQUE RIPPLE FOR VARIOUS NUMBER OF WINDING LAYER. $\hat{I}$=9 A

	1–layer	2–layer	4–layer
τ_{avg} (Nm)	9.9	10.3	10.1
$\Delta\tau$ (Nm)	1.7	1.1	0.4
	(17.2%)	(10.7%)	(3.9%)

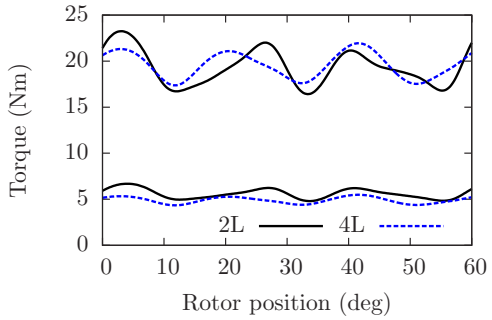

Fig. 19. Torque versus rotor position of FSIM with 2– and 4–layer windings

torque ripple are reported in Table IX. The average torque decreases with the 4–layer winding due to the lower winding factor according to (4).

Considering a 4–layer winding the torque ripple decreases significantly respect to the 2–layer winding. Nevertheless the torque ripple is still higher than 20% of the average torque also adopting a 4–layer winding. Since the analytical model is linear, the torque is proportional to the product of stator and rotor currents. Therefore, changing the currents the percentage torque ripple remains the same.

TABLE IX
FRACTIONAL SLOT INDUCTION MACHINE. AVERAGE TORQUE AND TORQUE RIPPLE FOR 2– AND 4–LAYER WINDINGS

	2–layer	4–layer
τ_{avg} (Nm)	22.6	19.6
$\Delta\tau$ (Nm)	7.6	4.6
	(33.6%)	(23.7%)

VI. CONCLUSIONS

In this paper the general theory of the multilayer m–phase winding is presented. General rules to design such a type of winding are given. Particular attention is paid to the feasibility of multilayer winding, showing that they are not convenient for any combinations of slots and poles. Examples of machine with more than three phases are included.

Several examples and applications have been included, considering also different machine types. The following considerations can be drawn:

SPM machine with 4–layer winding: the torque ripple is not significantly reduced, it is almost the same as the machine with 2– and 1–layer winding. Moreover only a slightly reduction of the rotor losses is found with respect to the 2–layer winding.

IPM machine with 4–layer winding: the torque ripple results significantly reduced, especially at high current when the machine results heavy saturated. This is particularly true when FS IPM machines are considered.

FSIM machine with 4–layer winding: the interaction of the MMF harmonics is reduced making feasible such a type of machine. In this case, however, a notable torque ripple is present also adopting the 4–layer winding.

VII. ACKNOWLEDGMENTS

The authors are very grateful to Eng. Mosè Castiello for his help and assistance during the experimental tests.

REFERENCES

[1] M. Liwschitz-Garik and C. C. Whipple, *Alternating–Current Machines*. Van Nostrand Company, 1961.

[2] R. Richter, *Lehrbuch der Wicklungen Elektrischer Machinen*, W. Bucherei, Ed. Karlsruhe: G. Braun, 1952.

[3] A. D. Gerlando, R. Perini, and M. Ubaldini, "High pole number, PM synchronous motor with concentrated coil armature windings," in *Proc. of International Conference on Electrical Machines, ICEM'04*, vol. CD Rom, Cracow, Poland, 2004, pp. 1–6.

[4] A. Di Gerlando, G. M. Foglia, R. Perini, and M. Ubaldini, "Design and operation aspects of field regulated PM synchronous machines with concentrated armature windings," in *Electric Machines and Drives, 2005 IEEE International Conference on*, May 15–18, 2005, pp. 1165–1172.

[5] K. Ito, K. Naka, M. Nakano, and M. Kobayashi, "Electric machine," US Patent US7 605 514, 20 Oct 2009.

[6] M. V. Cistelecan, F. J. T. E. Ferreira, and M. Popescu, "Three phase tooth-concentrated multiple-layer fractional windings with low space harmonic content," in *2010 IEEE Energy Conversion Congress and Exposition (ECCE)*, 2010, pp. 1399 –1405.

[7] M. Cistelecan, F. F. Ferreira, and M. Popescu, "Three-phase tooth-concentrated interspersed windings with low space harmonic content," in *in Proc. of ICEM 2010*, 2010.

[8] N. Bianchi, M. Dai Pré, L. Alberti, and E. Fornasiero, *Theory and Design of Fractional-Slot PM Machines*, Sponsored by the IEEE-IAS Electrical Machines Commitee, Ed. Padova: CLEUP (ISBN 978-88-6129-122-5), 2007.

[9] L. Alberti, E. Fornasiero, N. Bianchi, and S. Bolognani, "Rotor losses measurements in an axial flux permanent magnet machine," *IEEE Transactions on Energy Conversion*, vol. 26, no. 2, pp. 639 –645, june 2011.

[10] N. Bianchi and S. Bolognani, "Design techniques for reducing the cogging torque in surface-mounted PM motors," *IEEE Transactions on Industry Applications*, vol. 38, no. 5, pp. 1259–1265, Sep./Oct. 2002.

[11] L. Alberti, E. Fornasiero, and N. Bianchi, "Impact of the rotor yoke geometry on rotor losses in permanent magnet machines," in *Energy Conversion Congress and Exposition (ECCE), 2010 IEEE*, 2010, pp. 3486 –3492.

[12] E. Fornasiero, L. Alberti, N. Bianchi, and S. Bolognani, "Considerations on selecting fractional-slot windings," in *Energy Conversion Congress and Exposition (ECCE), 2010 IEEE*, 2010, pp. 1376 – 1383.

[13] N. Bianchi and E. Fornasiero, "Index of rotor losses in three-phase fractional-slot permanent magnet machines," *IET Electric Power Applications*, vol. 3, pp. 381–388, Sep. 2009.

[14] M. Barcaro, N. Bianchi, and F. Magnussen, "Analysis and tests of a dual three-phase 12-slot 10-pole permanent-magnet motor," *IEEE Transactions on Industry Applications*, vol. 46, no. 6, pp. 2355 – 2362, 2010.

[15] L. Alberti and N. Bianchi, "Analysis of asynchronous machines for direct drive wind power generation," in *Electric Machines and Drives Conference, 2009. IEMDC '09. IEEE International*, Miami, FL, May 2009, pp. 1838–1843.

[16] ——, "Design Of Fractional–Slot Induction Machine," in *IEEE Energy Conversion Congress and Exposition. ECCE.*, 2011, in press.